NASA TN D-1742

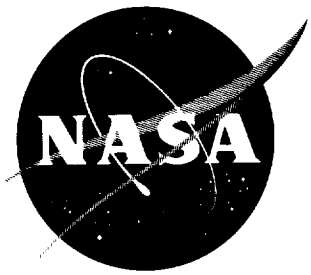

TECHNICAL NOTE

D-1742

A COMPARATIVE ANALYSIS OF CONVECTIVE HEAT TRANSFER IN A NUCLEAR ROCKET NOZZLE

By Harvey E. Neumann and Paula J. Bettinger

Lewis Research Center
Cleveland, Ohio

NATIONAL AERONAUTICS AND SPACE ADMINISTRATION
WASHINGTON

August 1963

NATIONAL AERONAUTICS AND SPACE ADMINISTRATION

TECHNICAL NOTE D-1742

A COMPARATIVE ANALYSIS OF CONVECTIVE HEAT TRANSFER IN A NUCLEAR ROCKET NOZZLE

By Harvey E. Neumann and Paula J. Bettinger

SUMMARY

A detailed analysis of the gas-side heat-transfer coefficient associated with a nuclear rocket nozzle is presented. The purpose of this study was to compare the predicted heat flux distributions obtained from conventional turbulent flow correlations with those obtained from boundary-layer theory. The effects of initial boundary-layer thickness, radial gradients of free-stream velocity, wall temperature distribution, and nozzle geometry on predicted heat flux are considered.

The results show that the heat-flux predictions from a Nusselt number correlation that comprehends radial gradients of free-stream velocity are in fair agreement with predictions from boundary-layer theory except in regions of the convergent section. The predicted heat-flux distribution in the convergent section is found to be sensitive to the initial boundary-layer development. At the throat and in the divergent section, the heat flux is found to be relatively independent of initial boundary-layer thickness. The nozzle geometry and distribution of mass flow per unit area strongly affected the heat-flux distribution. Differences in predicted heat flux of the order of 100 percent may be encountered in the divergent section when radial gradients of mass flow per unit area are ignored and one-dimensional flow is assumed.

INTRODUCTION

Currently, there is widespread interest in the open-cycle nuclear rocket as a propulsion device for space vehicles. A preliminary design study of nuclear rocket nozzle cooling with hydrogen as a working fluid is presented in reference 1. This study has shown that an extremely large heat flux may be expected in the region of the nozzle throat. This preliminary analysis has also shown that hydrogen, which is attractive as a coolant because of its high thermal conductivity and large heat capacity, may have a marginal coolant capability when used as a regenerative coolant. It is imperative, therefore, that, for marginal designs, accurate estimates of the local heat flux or the overall heat-transfer coefficient be predictable throughout the nozzle.

The local heat flux in a regeneratively cooled rocket nozzle is largely a function of the local gas-side heat-transfer coefficient. This coefficient is evaluated either from empirical correlations or from considerations of the bound-

dary layer. The empirical correlations, such as those contained in references 1 and 2, are generally of the form used for fully developed turbulent flow in pipes and, therefore, do not comprehend effects due to pressure gradient or boundary-layer growth.

A more fundamental approach to determining gas-side heat-transfer coefficients involves the determination of the boundary-layer characteristics. Methods for predicting the boundary-layer development and the heat transfer for flows with turbulent boundary layers and pressure gradients are presented in references 3 to 5. Although the boundary-layer approach is more fundamental, it is difficult to formulate all the boundary and initial conditions necessary to obtain a solution. In the nuclear rocket, the injection of the gas into the convergent section of the nozzle results in the generation of free-stream turbulence and eddies and affects the development of the boundary layer. The free-stream turbulence and the nature of the boundary layer can have large effects on heat transfer (refs. 6 to 8). No information is currently available on the nature of the flow in the convergent section of a nuclear-rocket nozzle. As a result, it is impossible to predict accurately the character of the boundary layer or its initial thickness in the convergent region of the nozzle near the reactor face.

Reference 2 shows that the mass flow per unit area adjacent to the boundary layer has a strong influence on the heat-flux distribution. Large gradients in mass flow rate per unit area in both the axial and radial directions exist in actual nozzle flows. The radial gradients of mass flow per unit area have been ignored in most preliminary analyses of nuclear rocket cooling. Since the nuclear rocket cooling appears to be critical, a more detailed analysis of the gas-side heat-transfer coefficients appears warranted and is presented in this report.

The method of reference 4, which is assumed representative of turbulent boundary-layer analyses has been subjected to several minor modifications and is used herein to obtain predictions of the heat-transfer distributions. Many of the assumptions in this method, however, have not been experimentally verified for conditions applicable to a nuclear rocket nozzle. Nevertheless, the results should at least have qualitative significance. Heat-transfer predictions obtained from the boundary-layer analysis presented herein are compared with experimental data from a heated-air facility in references 9 and 10. A comparison of the predicted heat-flux distributions obtained from the boundary-layer approach and predictions obtained from conventional turbulent-flow heat-transfer correlations is included. The qualitative effect of initial boundary-layer thickness on the heat-transfer distribution in a nozzle is determined by comparison of the results obtained for various values of initial boundary-layer thickness. Estimates of the errors in heat flux due to neglecting the radial gradients of mass flow rate per unit area are presented. The effect of wall temperature on heat-transfer coefficient was investigated by a comparison of the results obtained by using various wall temperature distributions. The nozzle geometries investigated were a Rao optimum-thrust bell-shaped nozzle and a 15° conical nozzle.

SYMBOLS

C_f local coefficient of skin friction

d diameter of nozzle

h enthalpy

h_g heat-transfer coefficient, $h_g \equiv \frac{q_w}{h_{ad} - h_w}$

M Mach number

m molecular weight

Pr Prandtl number

p pressure

q heat flux

r radius of nozzle

s entropy

t temperature

u velocity in x-direction

X axial distance, defined to be positive in divergent section and negative in convergent section

x distance along wall in direction of flow

y distance normal to wall

γ isentropic exponent, $\gamma \equiv \left(\frac{\partial \ln p}{\partial \ln \rho}\right)_s$

Δ thermal boundary-layer thickness

δ velocity boundary-layer thickness

δ^* boundary-layer displacement thickness, defined by eq. (3b)

θ boundary-layer momentum thickness, defined by eq. (3a)

λ boundary-layer shape factor, $\lambda \equiv \varphi/[\theta(\Delta/\delta)^{-8/7}]$

μ viscosity

ρ density

φ boundary-layer energy thickness, defined by eq. (3c)

Subscripts:

ad adiabatic wall

b	boundary-layer computation using axisymmetric $\rho_e u_e$ distribution
e	isentropic free stream adjacent to boundary layer
i	initial value
ref	reference condition
t	throat
w	wall
ϵ	area ratio
0	stagnation condition

METHOD OF ANALYSIS

The heating of a nuclear rocket nozzle occurs by a combination of convective heat transfer from the high-temperature propellant and thermal and gamma radiation from the reactor face. The analysis of reference 1 indicates that gamma heating is about one or more orders of magnitude smaller than the total heat flux. The effects of thermal radiation are shown in reference 1 to be a strong function of the stagnation pressure and are important only in the convergent section of the nozzle. The heat flux due to thermal radiation in the divergent section is about an order of magnitude smaller than in the convergent section. In this analysis, gamma-particle and thermal radiation are neglected, and only convective heat transfer is considered. In the design of coolant passages for a nuclear rocket nozzle, however, the contribution of radiation to the total heat flux should not be ignored.

In a nuclear rocket nozzle, the Reynolds numbers are generally sufficiently large so that turbulent boundary layers are expected to persist throughout the nozzle. In addition, transitional Reynolds numbers should be lower than normal because of the free-stream turbulence created by the ejection of the hot gases from the reactor core. It is assumed herein, therefore, that a fully developed turbulent profile exists in the boundary layer throughout the nozzle.

The method of reference 4 for determining the compressible turbulent boundary-layer development has been subjected to several minor modifications and is used in this analysis. The pertinent equations and assumptions are summarized, and all modifications are presented. This method (ref. 4) is based on approximate solutions to both the integral-momentum and integral-energy equations. The integral equations for steady axisymmetric flow with an isentropic main stream and no chemical reactions in the boundary layer become:

Momentum:

$$\frac{d\theta}{dx} + \left[\left(2 + \frac{\delta^*}{\theta}\right)\frac{1}{u_e}\frac{du_e}{dx} + \frac{1}{\rho_e}\frac{d\rho_e}{dx} + \frac{1}{r}\frac{dr}{dx}\right]\theta = \frac{C_f}{2} \tag{1}$$

Energy:

$$\frac{d\varphi}{dx} + \varphi \frac{d}{dx}\left[\ln r\rho_e u_e(h_{0,e} - h_w)\right] = \frac{q_w}{\rho_e u_e(h_{0,e} - h_w)} \tag{2}$$

where

$$\theta \equiv \int_0^\infty \frac{\rho u}{\rho_e u_e}\left(1 - \frac{u}{u_e}\right)dy$$

$$\delta^* \equiv \int_0^\infty \left(1 - \frac{\rho u}{\rho_e u_e}\right)dy$$

$$\varphi \equiv \int_0^\infty \frac{\rho u}{\rho_e u_e}\left(1 - \frac{h_0 - h_w}{h_{0,e} - h_w}\right)dy$$

The values of the boundary-layer thickness parameters are dependent only on the variation of both the velocity and enthalpy within the boundary layers. The integrations, therefore, need only be evaluated from the wall to the point where neither the velocity nor the stagnation enthalpy differ from their respective free-stream values. Hence, the thickness parameters become

$$\theta = \int_0^\zeta \frac{\rho u}{\rho_e u_e}\left(1 - \frac{u}{u_e}\right)dy \tag{3a}$$

$$\delta^* = \int_0^\zeta \left(1 - \frac{\rho u}{\rho_e u_e}\right)dy \tag{3b}$$

$$\varphi = \int_0^\zeta \frac{\rho u}{\rho_e u_e}\left(1 - \frac{h_0 - h_w}{h_{0,e} - h_w}\right)dy \tag{3c}$$

where $\zeta = \delta$ if $\Delta/\delta \leq 1$ and $\zeta = \Delta$ if $\Delta/\delta \geq 1$. To complete the formulation of the problem, it is necessary to specify (1) an additional relation between the skin friction coefficient and the heat flux, (2) a wall friction relation, and (3) enthalpy and velocity distributions through the boundary layer. Knowledge of the inviscid flow characteristics in the layer adjacent to the boundary layer and the axial wall enthalpy distribution will then permit solution of equations (1) and (2) to obtain the heat-transfer distribution throughout the nozzle.

It is assumed, as in reference 4, that the boundary layer is characterized by variations in velocity and enthalpy such that Reynold's analogy is valid and

the local skin friction coefficients are the same as those that would exist on a flat plate for the same boundary-layer thickness. The relation for the Reynolds analogy between momentum transfer and heat transfer, as derived in reference 4, is

$$\frac{q_w}{\rho_e u_e (h_{0,e} - h_w)} = \frac{\frac{C_f}{2}}{\left(\frac{\Delta}{\delta}\right)^{1/7} Pr_e^a} \tag{4}$$

where a is 0.62 for $\rho_e u_e \delta/\mu_e$ near 10^5, 0.46 for $\rho_e u_e \delta/\mu_e$ near 10^4, and 0.36 for $\rho_e u_e \delta/\mu_e$ near 10^3.

The wall friction relation, identical to that used in reference 4, is given by

$$\frac{C_f}{2} = 0.0228\, \sigma \left(\frac{\mu_{0,e}}{\rho_e u_e \delta}\right)^{1/4} \tag{5}$$

where

$$\sigma = \left[\frac{1}{2}\frac{t_w}{t_{0,e}}\left(1 + \frac{\gamma - 1}{2} M_e^2\right) + \frac{1}{2}\right]^{-0.60} \left(1 + \frac{\gamma - 1}{2} M_e^2\right)^{-0.15}$$

The velocity and enthalpy distributions through the boundary layer are required to determine boundary-layer shape parameters. It is assumed herein that the velocity is described by a one-seventh power-law distribution of the form

$$\left(\frac{y}{\delta}\right)^{1/7} = \frac{u}{u_e} \tag{6}$$

The enthalpy distribution is similar to that used in reference 4. The difference between the stagnation enthalpy and the enthalpy at the wall is also assumed herein to vary as a one-seventh power law of the form

$$\left(\frac{y}{\Delta}\right)^{1/7} = \frac{h_0 - h_w}{h_{0,e} - h_w} \tag{7}$$

The density variation within the boundary layer that is required to evaluate the boundary-layer thickness parameters is determined from the static-pressure and enthalpy distributions. The static pressure remains constant across the boundary layer at any axial location. The static-enthalpy variation, however, depends on the relative thickness of the thermal and velocity layers and the variation of velocity and stagnation enthalpy within the boundary layer. Therefore, by using the definition of stagnation enthalpy and equations (6) and (7), the static-enthalpy variation through the boundary layer can be expressed as

$$\frac{h}{h_e} = 1 - C_0\left(1 - \frac{h_w}{h_{0,e}}\right)\left[1 - \left(\frac{y}{\Delta}\right)^{1/7}\right]\frac{h_{0,e}}{h_e} + C_1\left(\frac{h_{0,e}}{h_e} - 1\right)\left[1 - \left(\frac{y}{\delta}\right)^{2/7}\right] \tag{8a}$$

where

$$C_0 \equiv 1,\ C_1 \equiv 1 \qquad \text{for} \quad y < \delta \quad \text{and} \quad y < \Delta$$

$$C_0 \equiv 0,\ C_1 \equiv 1 \qquad \text{for} \quad \Delta < y < \Delta$$

$$C_0 \equiv 1,\ C_1 \equiv 0 \qquad \text{for} \quad \delta < y < \Delta$$

The density at any point is then defined by the corresponding static pressure and enthalpy and must be obtained from thermodynamic tables or charts. For the special case of constant specific heat and frozen composition, variation across the boundary layer can be expressed as the explicit function

$$\frac{\rho_e}{\rho} = \frac{t}{t_e} = 1 - C_0\left(1 - \frac{t_w}{t_{0,e}}\right)\left[1 - \left(\frac{y}{\Delta}\right)^{1/7}\right]\left(1 + \frac{\gamma - 1}{2} M_e^2\right)$$

$$+ C_1 \frac{\gamma - 1}{2} M_e^2\left[1 - \left(\frac{y}{\delta}\right)^{2/7}\right] \tag{8b}$$

Equations (1) to (8a) are sufficient to describe the heat-transfer and the boundary-layer development; however, for convenience a boundary-layer shape parameter is introduced in the energy relation (eq. (2)) (see ref. 4). Because of this shape parameter, the energy equation is primarily dependent on the single dependent variable Δ/δ. By using the definition of the shape factor λ and equation (4), the energy relation (eq. (2)) becomes

$$\frac{\left(\frac{\Delta}{\delta}\right)^{9/7}}{dx} + \frac{9}{8}\left(\frac{\Delta}{\delta}\right)^{9/7} \frac{d \ln[\rho_e u_e r \theta \lambda (h_{0,e} - h_w)]}{dx} = \frac{9}{16} \frac{C_f}{Pr_e^a \lambda \theta} \tag{9}$$

where

$$\lambda = \frac{\varphi}{\theta}\left(\frac{\Delta}{\delta}\right)^{-8/7}$$

Before a solution can be effected, several initial conditions must be specified. Quantitative estimates of the thicknesses of the thermal and velocity layers at the entrance of the nozzle must be made to initiate the numerical calculations. The set of relations from which the heat-transfer and boundary-layer development are obtained is composed of the axial distributions of temperature and enthalpy along the wall, the coordinates of the wall, the axial distributions of velocity, the thermodynamic properties of the inviscid fluid immediately adjacent to the boundary layer, and equations (1) and (5) to (9). The solution is obtained by following the computational procedure outlined in reference 4.

CALCULATIONAL PROCEDURE

The turbulent boundary-layer method presented in the previous section was used herein to predict the gas-side heat transfer in a nuclear rocket nozzle.

The propellant considered was hydrogen. A stagnation pressure and temperature of 375 pounds per square inch absolute and 4460° R, respectively, were assumed at the discharge from the reactor. At these conditions, very little dissociation of the hydrogen can occur; and, therefore, a constant molecular composition was assumed throughout the expansion process within the nozzle. The method and thermodynamic data presented in reference 11 were used to generate the necessary properties of the gas in the expansion process. The transport properties used herein were obtained from reference 12.

Two nozzle shapes were considered: a bell contour and a 15° conical contour. The convergent sections of the two nozzles were identical. The contour of the bell-shaped nozzle is shown in figure 1. The length of the divergent section (fig. 1) is 88 percent of the length of a 15° conical nozzle having an equal area ratio. An axisymmetric-characteristics solution was used to design the nozzle contour and to determine the associated flow distribution in the divergent section of the bell-shaped contour. The characteristics solution was based on the optimization technique of reference 13 and used the method of reference 14 to obtain the transonic initial conditions. One-dimensional flow was assumed to exist in the convergent sections of both the bell-shaped nozzle and the conical nozzle. The assumed flow distribution in the region of the throat in the conical nozzle deviated from one-dimensional flow and was similar to the experimental pressure distribution presented in reference 15. The flow distribution in the divergent section of the conical nozzle was assumed to be one dimensional.

Viscous computations were made with the assumed flow distributions to determine the boundary-layer development and associated heat transfer for both nozzles. For the purposes of comparison, the boundary-layer computations were recalculated with one-dimensional flow being assumed throughout. The effect of wall temperature on heat transfer was studied by considering different arbitrary axial distributions and levels of wall enthalpy. The arbitrary axial variation of wall enthalpy given in figure 2 and the enthalpies corresponding to constant wall temperatures of 1000°, 1500°, and 2000° R were assumed.

It is currently impossible to predict accurately the initial characteristics of the boundary layer near the reactor face in a nuclear rocket; however, a qualitative study of the effect of initial boundary-layer thickness on heat-transfer coefficient in the region of the throat and the divergent portion of the nozzle can be obtained by varying the initial thickness. Three arbitrary initial conditions were therefore assumed. For the first set of conditions, the boundary layer was assumed to start at the nozzle entrance with zero thickness. Immediate transition to a fully developed turbulent profile was then assumed. For comparative purposes, viscous calculations were also made by assuming that the boundary layer started with a fully developed turbulent profile and with initial thicknesses of 0.09 and 0.34 inch.

As specified in the introduction, the results from the boundary-layer calculations were compared to conventional heat-transfer coefficient correlations. Most correlations for rocket nozzles have the form of the conventional Nusselt number correlation for turbulent flow in a pipe. Differences in correlations are primarily concerned with the manner in which the thermodynamic properties are applied, the values of the empirical coefficient and exponents involved, and the nature of the driving energy potential. References 2 and 10 each contain a typi-

cal Nusselt correlation. The correlation presented in reference 10 is used herein as the basis of comparison with the boundary-layer calculations. This Nusselt correlation is based on an enthalpy driving potential and gas transport properties based on a reference condition. The correlation therefore can be expressed as

$$h_g \equiv \frac{0.026(\rho_e u_e)^{0.8} \mu_{ref}^{0.2}}{d^{0.2} Pr_{ref}^{0.667}} \left(\frac{t_e/m_e}{t_{ref}/m_{ref}} \right)^{0.8} \tag{10}$$

where

$$h_g \equiv \frac{q_w}{h_{ad} - h_w}$$

The terms μ_{ref}, Pr_{ref}, and t_{ref}/m_{ref} are evaluated at the local static pressure and a reference enthalpy given by

$$h_{ref} = h_e + \frac{1}{2}(h_w - h_e) + 0.22\, Pr_{ref}^{1/3} (h_{0,e} - h_e) \tag{11a}$$

The adiabatic enthalpy term in the definition of the film coefficient is obtained from

$$h_{ad} = h_e + Pr_{ref}^{1/3} (h_{0,e} - h_e) \tag{11b}$$

As in reference 10, the heat-transfer coefficient from the Nusselt correlation is evaluated for the conditions of both one-dimensional and two-dimensional axisymmetric flows.

RESULTS AND DISCUSSION

Typical Axial Variations of Heat Flux

The local heat flux varies appreciably throughout a nozzle with the maximum flux usually appearing slightly upstream of the geometric throat. A typical variation of heat flux, as obtained from the boundary-layer calculations, is shown in figure 3. A relatively large heat flux is predicted only in the throat region. This is to be expected because of the primary dependence of heat-transfer coefficient on mass flow per unit area. This effect is discussed in the section Effect of Flow Distribution.

The heat flux is about an order of magnitude lower in the convergent and divergent sections than at the nozzle throat. The lower values of heat flux in the convergent and divergent sections make these sections easy to cool. When the entire nozzle is regeneratively cooled, however, several situations can exist that require accurate prediction throughout the nozzle.

First, the total heat transferred to the coolant is not small in the divergent portion of a nozzle because of the large surface areas involved. The total energy transferred to the wall per inch of coolant passage in the divergent section may be about 25 to 50 percent of the energy transferred at the throat if the

area ratio is sufficiently large. It is possible therefore to utilize the divergent section of a regeneratively cooled nozzle as a heat exchanger in a subsystem such as the turbine drive. Errors in the prediction of heat flux in the nozzle skirt could thus have a large effect on the expected performance of the subsystem.

Second, in a regeneratively cooled nozzle, the temperature of the coolant at any axial position is dependent on the total heat previously added to the coolant. Thus, it is possible for errors in the prediction of heat flux in the divergent section to be manifested in regions of the nozzle that are more difficult to cool. Hence, for marginal cooling designs and for applications where the nozzle coolant passages are used as a heat exchanger, the total heat transferred to the wall in the divergent section of the nozzle can be very important.

Effect of Initial Boundary Layer Thickness

It is currently impossible to predict accurately the thickness of the velocity and thermal boundary layers at the entrance to a nuclear rocket nozzle. In order to evaluate the effect of the initial boundary-layer thickness on heat transfer, however, the axial distributions of heat flux in the bell-shaped nozzle were computed for three arbitrary values of initial boundary-layer thickness. A comparison of the results in the convergent section of the nozzle is shown in figure 4. The heat-flux distribution obtained from a Nusselt correlation is also presented. Figure 4 shows that, in the convergent section of the nozzle, the heat flux computed from a boundary-layer analysis is rather sensitive to the initial thickness. A difference in heat flux at the entrance of the nozzle of about 35 percent is noted in the comparison of a 0.09-inch initial thickness and a 0.34-inch initial thickness. Near the nozzle throat, the sensitivity to initial boundary-layer thickness diminishes. A difference of only 3 percent in heat flux is noted at the throat. Although it is impossible to predict accurately the heat transfer in the convergent section without a knowledge of the entrance conditions, meaningful predictions appear to be possible in the throat region from a boundary-layer analysis.

The values of heat flux obtained from the Nusselt correlation given by equation (10) are lower than those obtained from the boundary-layer analysis throughout the convergent section. These differences are due to the inability of the Nusselt correlation to comprehend completely boundary-layer development effects. Qualitatively, similar experimental results have been obtained with chemical rockets in reference 16 where heat-transfer data are presented for a range of contraction ratios. For the largest contraction ratio, the experimental values of heat flux (ref. 16) were substantially higher in the chamber than those predicted by a Nusselt correlation technique; however, due to the effects of combustion and injection on the data of reference 16, no quantitative comparisons can be made to assess the ability of the boundary-layer approach to predict heat flux in this case.

At the throat of a nozzle, the boundary layer is very thin and its thickness increases with axial distance throughout the divergent section. It would be expected, therefore, that the initial boundary-layer thickness would have little effect on the heat flux in the divergent section of the nozzle. This is substan-

tiated by a comparison of the heat-flux distributions for various initial thicknesses. The effect of initial boundary-layer thickness is shown in figure 5 in a magnified form by the deviation of the heat flux obtained with finite initial thickness from that value obtained using an initial thickness of zero. The maximum difference for the three cases considered is 3 percent, which occurs at the throat. In reference 10, the effect of initial boundary-layer thickness on the heat flux in the divergent section was studied for a different inlet geometry and flow condition. A maximum effect of 13 percent was observed. It appears, therefore, that the effect of initial boundary-layer thickness on heat flux is somewhat dependent on the characteristics of the flow at the inlet.

Effect of Flow Distribution

The local heat-transfer coefficient is largely a function of the local mass flow per unit area $\rho_e u_e$ which is determined from the characteristics of the inviscid flow adjacent to the boundary layer. Two techniques are generally available for determining $\rho_e u_e$. The first is to relate $\rho_e u_e$ to the mass flow rate and local area through the one-dimensional continuity relation. This technique is probably the most common primarily because of its simplicity. The second technique is to obtain $\rho_e u_e$ from axisymmetric calculations for the region adjacent to the boundary layer. In the convergent region of a nozzle, the flow is usually very close to being one dimensional except for nozzles with very large contraction angles. Figure 6 shows that the flow departs greatly from the one-dimensional case in the divergent region of the bell-shaped nozzle. In the throat region, the peak $\rho_e u_e$ for the axisymmetric case appeared upstream of the location of the maximum value for the one-dimensional case. The location of the maximum $\rho_e u_e$ deviates from the geometric throat as a result of the nonplanar sonic surface. In the divergent section immediately downstream of the throat, the axisymmetric values of $\rho_e u_e$ are lower than the corresponding one-dimensional values. This trend reverses, however, at an area ratio of about 4, and the axisymmetric values of $\rho_e u_e$ are then larger than the one-dimensional values. The heat flux should have a similar axial distribution.

The predicted peak heat flux (fig. 3) is located at a point slightly upstream of the geometric throat; this deviation is a result of both the $\rho_e u_e$ distribution and the axial variation of the fluid properties and boundary-layer thickness parameters.

In figure 7 the divergent section heat-flux distributions resulting from the one-dimensional $\rho_e u_e$ and the axisymmetric $\rho_e u_e$ distributions are compared. Both the results from the boundary-layer theory and the Nusselt correlation for each $\rho_e u_e$ distribution are included in the comparison. From a comparison of the results presented in figures 6 and 7, it can be concluded that the heat-flux distributions and the $\rho_e u_e$ distributions follow similar trends.

The heat-flux distributions (fig. 7) are shown in figure 8 as deviations from the heat-flux distribution obtained from the boundary-layer calculation based on an axisymmetric $\rho_e u_e$ distribution. Results from the axisymmetric boundary-layer theory are significantly different from those for the one-dimensional boundary-layer approach throughout the divergent portion of the nozzle. The one-dimensional results are about 100 percent higher than the axisym-

metric results at the axial location of the nozzle where the expansion angle is a maximum. Near the exit of the nozzle, the axisymmetric results generally yield heat fluxes that are much greater than those obtained from the one-dimensional approach. For large exit area ratios the differences can amount to about 50 percent. Similar differences exist in the comparison of results from the Nusselt correlation with the two different flow distributions. Although the largest differences in heat flux occur in regions of the nozzle where the magnitude of the flux is not a maximum, the differences can, in certain cases, be significant. As previously discussed, accurate estimates of the heat-transfer coefficient in the divergent section may be necessary in nozzles where cooling is extremely marginal or where the nozzle skirt is utilized as a heat exchanger.

From the comparisons presented in figure 8, it is apparent that the two Nusselt number correlations agree with the corresponding results from the boundary-layer calculations to within about 20 to 40 percent. For the calculations that use axisymmetric values of $\rho_e u_e$, the difference in the two methods of evaluating the heat-transfer coefficient is relatively constant throughout the nozzle. The results from the Nusselt number correlation are about 20 percent lower than the results from the boundary-layer calculations. Although the Nusselt correlation approach does not include boundary-layer growth parameters, based on an axisymmetric value of $\rho_e u_e$, it should be adequate in the divergent section for preliminary cooling design of bell-shaped nozzles, if the cooling is not critical. It may be desirable to change the coefficient to some value other than the 0.026, which was used in these calculations. The desired value will need to be determined experimentally.

Geometry Effects

The previous discussion has been concerned with a fixed bell-shaped nozzle contour. Any change in nozzle geometry affects the flow distribution and, hence, results in a change in the heat flux. A correction factor for geometric scale effects on heat transfer is derived in reference 4 for the idealized case of a family of conical nozzles with one-dimensional flow throughout. For the more generalized case of axisymmetric flow in a bell-shaped nozzle, no general geometric correction factor is known. The heat-transfer distribution for each bell-shaped contour must be individually evaluated.

When a constant area section is added upstream of the converging section of a nozzle, the boundary-layer thickness will increase with axial length in the constant area section. The boundary-layer thickness at the beginning of the converging section would be thicker than that of the nozzle without the constant area section. As discussed previously, the larger boundary-layer thickness at the beginning of the converging section will result in a reduction in heat-transfer coefficient throughout the nozzle. The heat-transfer coefficient in the divergent section will not be as greatly affected as the coefficient in the convergent section.

The effect of contraction ratio on heat flux was investigated by considering the case where the nozzle of figure 1 was truncated at a contraction ratio of 4.3. The heat-flux distribution associated with the truncated nozzle is presented in figure 9 as the deviations from the results for the untruncated nozzle

with a contraction ratio of 15. Both heat-flux distributions were obtained from the boundary-layer analysis in which an axisymmetric $\rho_e u_e$ distribution was used and the initial boundary-layer thickness was assumed to be zero. The results show a relatively small effect of contraction ratio throughout the nozzle except near the entrance. Reducing the contraction ratio increased the heat flux by about 30 percent at the entrance of the nozzle. The peak heat flux (near the throat) was only increased by about 6 percent, however. The values at the throat presented in figure 9 are qualitatively similar to those obtained from the theory of reference 17; however, this theory predicted about a 13 percent increase in peak heat flux with a decrease in contraction ratio from 15 to 4.3. Inasmuch as current nuclear rocket nozzles have contraction ratios of the order of 15, the effect of contraction ratio on heat transfer should be small.

Geometric changes in the divergent section of a nozzle can drastically alter the axial distribution of mass flow per unit area resulting also in a change in the heat-flux distribution. The variations of heat flux in the bell-shaped nozzle of figure 1 and in a 15° conical nozzle are compared in figure 10. The convergent section and entrance conditions were held fixed in the comparison. In addition, the wall enthalpy was held constant at a value corresponding to a wall temperature of 2000° R. Although there was a drastic change in nozzle geometry, figure 10 shows that the heat flux obtained from the boundary-layer calculations retained essentially the same functional dependence on mass flow per unit area. There is a maximum difference of 12 percent between the results for the conical and bell-shaped nozzles. Changes in pressure gradient along the wall and boundary-layer growth parameters resulting from a change in the shape of the divergent section of a nozzle, therefore, appear, on the basis of this comparison, to have only a secondary effect on the heat flux. The predominant influence on the heat flux is the mass flow per unit area that exists adjacent to the boundary layer.

Effect of Wall Temperature

The effect of wall temperature or wall enthalpy on heat transfer was evaluated by varying the axial distribution of wall temperature while holding all other parameters fixed. Three levels of constant wall enthalpy corresponding to wall temperatures of 1000°, 1500°, and 2000° R were considered. In addition, the axial distribution of wall enthalpy presented in figure 2 was arbitrarily assumed to facilitate evaluation of the effects of wall enthalpy gradient. The predicted heat fluxes associated with each wall enthalpy distribution were determined for the bell-shaped nozzle from boundary-layer theory with an axisymmetric $\rho_e u_e$ distribution. The results of the comparison are presented in figure 11 as axial variations of the ratio of the predicted heat-transfer coefficient to the predicted heat-transfer coefficient obtained with a constant 2000° R wall temperature.

The axial locations where the wall temperature reached values of 1000°, 1500°, and 2000° R are indicated on the results from the case with a variable temperature distribution. A comparison of results at these points with the results at comparable conditions for the constant wall temperatures indicates only a 2- to 5-percent effect due to wall temperature gradient. The effect on heat-transfer coefficient of changes in wall temperature level is shown to be much

larger than the wall temperature gradient effects. A decrease in wall temperature from 2000° to 1500° R results in a predicted increase in heat-transfer coefficient of about 10 percent in the divergent section of the nozzle. Near the throat and in the convergent section the resultant increase is only about 5 percent. Similar increases in heat-transfer coefficient are noted in figure 11 for further reductions in wall temperature level.

The wall temperature effects on predicted heat-transfer coefficient presented in figure 11 are largely a consequence of the dependence of the assumed friction law (eq. (5)) on wall temperature. Inasmuch as little friction data are available for the conditions pertinent to a nuclear rocket nozzle, it is difficult to judge the ability of the assumed friction law to comprehend wall temperature effects. The quantitative predictions of the effect of wall temperature on skin friction and, hence, heat-transfer coefficient, may be in error. More experimental friction and heat-transfer data are therefore needed.

SUMMARY OF RESULTS

A detailed analysis of the gas-side heat-transfer coefficient associated with a nuclear rocket nozzle is presented. Results from a boundary-layer analysis and a conventional Nusselt number correlation are compared. The following results were obtained in this investigation:

1. The effect of the initial boundary-layer thickness on gas-side heat-transfer coefficient is large near the entrance of the nozzle but diminishes downstream in the convergent section. At the throat and in the divergent section, the heat flux is relatively independent of initial boundary-layer thickness. The conventional Nusselt number correlations cannot be expected to give accurate predictions of heat flux in the convergent section because the correlation neglects the effects of initial boundary-layer thickness.

2. Results from the boundary-layer theory and the conventional Nusselt number correlations indicate that the local heat-transfer coefficient is predominantly a function of the local mass flow per unit area. In a bell-shaped nozzle, the mass flow per unit area and, hence, the predicted heat flux, depart greatly from that obtained by using techniques involving conventional one-dimensional flow assumptions. Differences in predicted heat flux of the order of 100 percent may be encountered in the divergent section when a one-dimensional value of $\rho_e u_e$ is used instead of the axisymmetric value.

3. Heat-flux predictions from the Nusselt number correlation, based on values of $\rho_e u_e$ at the wall, are in fair agreement with the results from the boundary-layer calculations except in regions of the convergent section.

4. Changes in the geometry of the nozzle will change the distribution of the mass flow per unit area and, hence, the heat-flux distribution. Results from a numerical comparison presented herein indicate that changes in the pressure gradient along the wall and the boundary-layer growth parameters resulting from the change in geometry appear to have only a secondary effect on the predicted heat flux.

5. The axial gradient of wall temperature was found to have a 2- to 5-percent effect on predicted heat-transfer coefficient for the particular wall temperature variation considered. A decrease in wall temperature level of 500° R resulted in an increase of about 5 to 15 percent in predicted heat-transfer coefficient. This effect of wall temperature was found to be primarily a result of the dependence of the assumed friction law on wall temperature. Experimental verification of the effect of wall temperature on heat-transfer coefficient is therefore required.

Lewis Research Center
National Aeronautics and Space Administration
Cleveland, Ohio, April 26, 1963

REFERENCES

1. Robbins, William H., Bachkin, Daniel, and Medeiros, Arthur A.: An Analysis of Nuclear-Rocket Nozzle Cooling. NASA TN D-482, 1960.

2. Bartz, Donald R.: A Simple Equation for Rapid Estimation of Rocket Nozzle Convective Heat Transfer Coefficients. Jet Prop., vol. 21, no. 1, Jan. 1957, pp. 49-51.

3. Cohen, Nathaniel B.: A Method for Computing Turbulent Heat Transfer in the Presence of a Streamwise Pressure Gradient for Bodies in High-Speed Flow. NASA MEMO 1-2-59L, 1959.

4. Bartz, Donald R.: An Approximate Solution of Compressible Turbulent Boundary-Layer Development and Convective Heat Transfer in Convergent-Divergent Nozzles. Trans. ASME, vol. 77, no. 8, Nov. 1955, pp. 1235-1245.

5. Reshotko, Eli, and Tucker, Maurice: Approximate Calculation of the Compressible Turbulent Boundary Layer with Heat Transfer and Arbitrary Pressure Gradient. NACA TN 4154, 1957.

6. Sugawara, Sugao, Takashi, Sato, Komatsu, Hiroyasu, and Hiroichi, Osaka: The Effect of Free-Stream Turbulence on Heat Transfer from a Flat Plate. NACA TM 1441, 1958.

7. Kestin, J., and Maeder, P. F.: Influence of Turbulence on Transfer of Heat from Cylinders. NACA TN 4018, 1957.

8. Van Der Hegge Zijnen, B. G.: Heat Transfer from Horizontal Cylinders to a Turbulent Air Flow. Appl. Sci. Res., sec. A, vol. 7, nos. 2-3, 1958, pp. 205-223.

9. Fortini, Anthony, and Ehlers, Robert C.: A Comparison of Experimental to Predicted Heat Transfer in a Bell Nozzle with Upstream Flow Disturbances. NASA TN D-1743, 1963.

10. Benser, W. A., and Graham, R. W.: Hydrogen Convective Cooling of Rocket Nozzles. Paper 62-AV-22, ASME, 1962.

11. Huff, Vearl N., Gordon, Sanford, and Morrell, Virginia E.: General Method and Thermodynamic Tables for Computation of Equilibrium Composition and Temperature of Chemical Reactions. NACA Rep. 1037, 1951. (Supersedes NACA TN's 2113 and 2161.)

12. Svehla, Roger A.: Estimated Viscosities and Thermal Conductivities of Gases at High Temperatures. NASA TR R-132, 1962.

13. Rao, G. V. R.: Exhaust Nozzle Contour for Optimum Thrust. Jet Prop., vol. 28, no. 6, June 1958, pp. 377-382.

14. Sauer, R.: General Characteristics of the Flow Through Nozzles at Near Critical Speeds. NACA TM 1147, 1947.

15. Massier, P. F., Gier, H. L., and Harper, E. Y.: Heat Transfer and Fluid Mechanics. Space Programs Summary 37-16, vol. IV, June 1-Aug. 1, 1962, Jet Prop. Lab., C.I.T., Aug. 31, 1962.

16. Welsh, William E., Jr., and Witte, Arvel B.: A Comparison of Analytical and Experimental Local Heat Fluxes in Liquid-Propellant Rocket Thrust Chambers. Tech. Rep. 32-43, Jet Prop. Lab., C.I.T., Feb. 1, 1961.

17. Mayer, Ernest: Analysis of Convective Heat Transfer in Rocket Nozzles. ARS Jour., vol. 31, no. 7, July 1961, pp. 911-916.

Figure 1. - Bell-shaped nozzle contour.

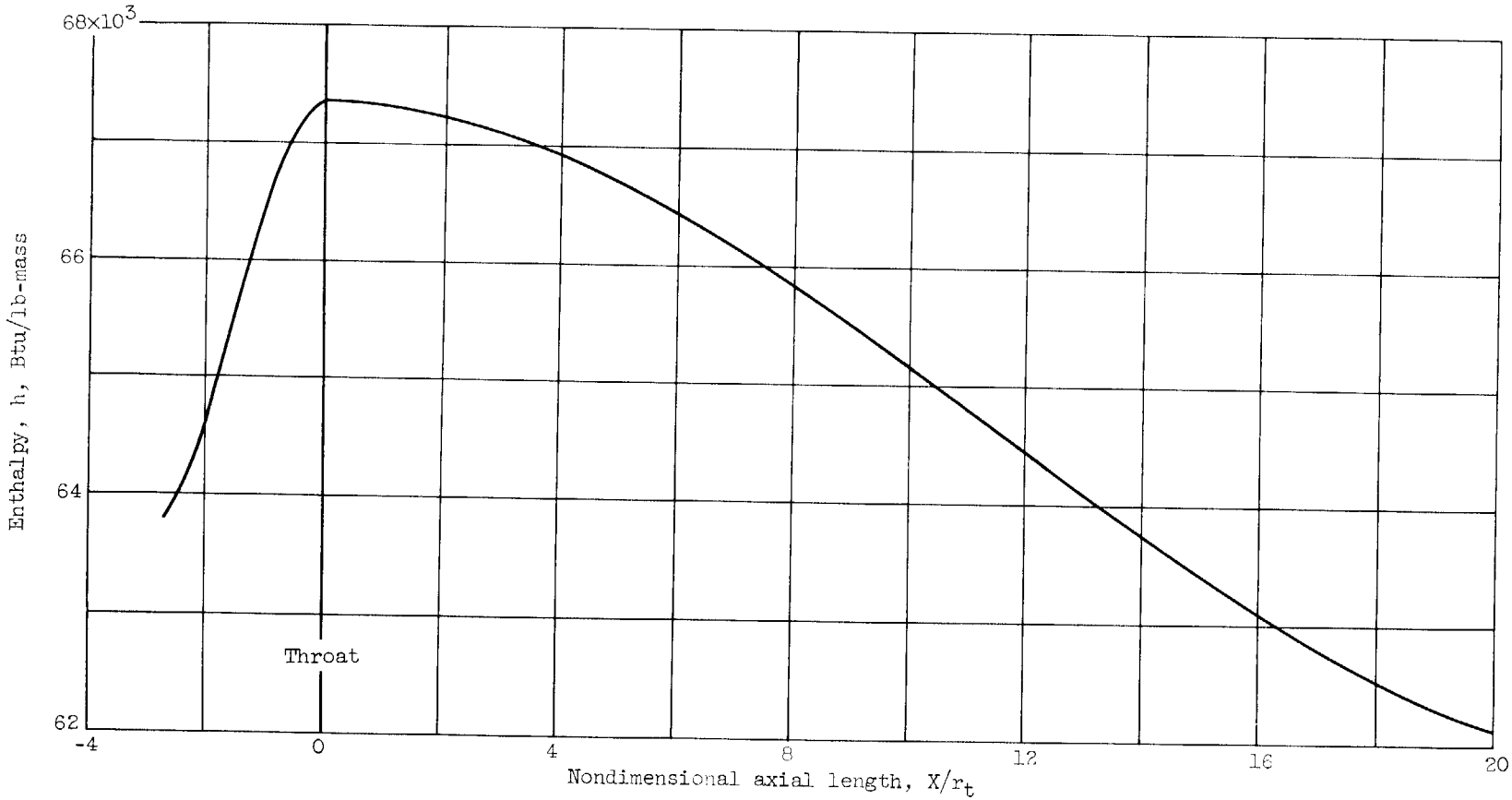

Figure 2. - Assumed axial distribution of enthalpy at wall.

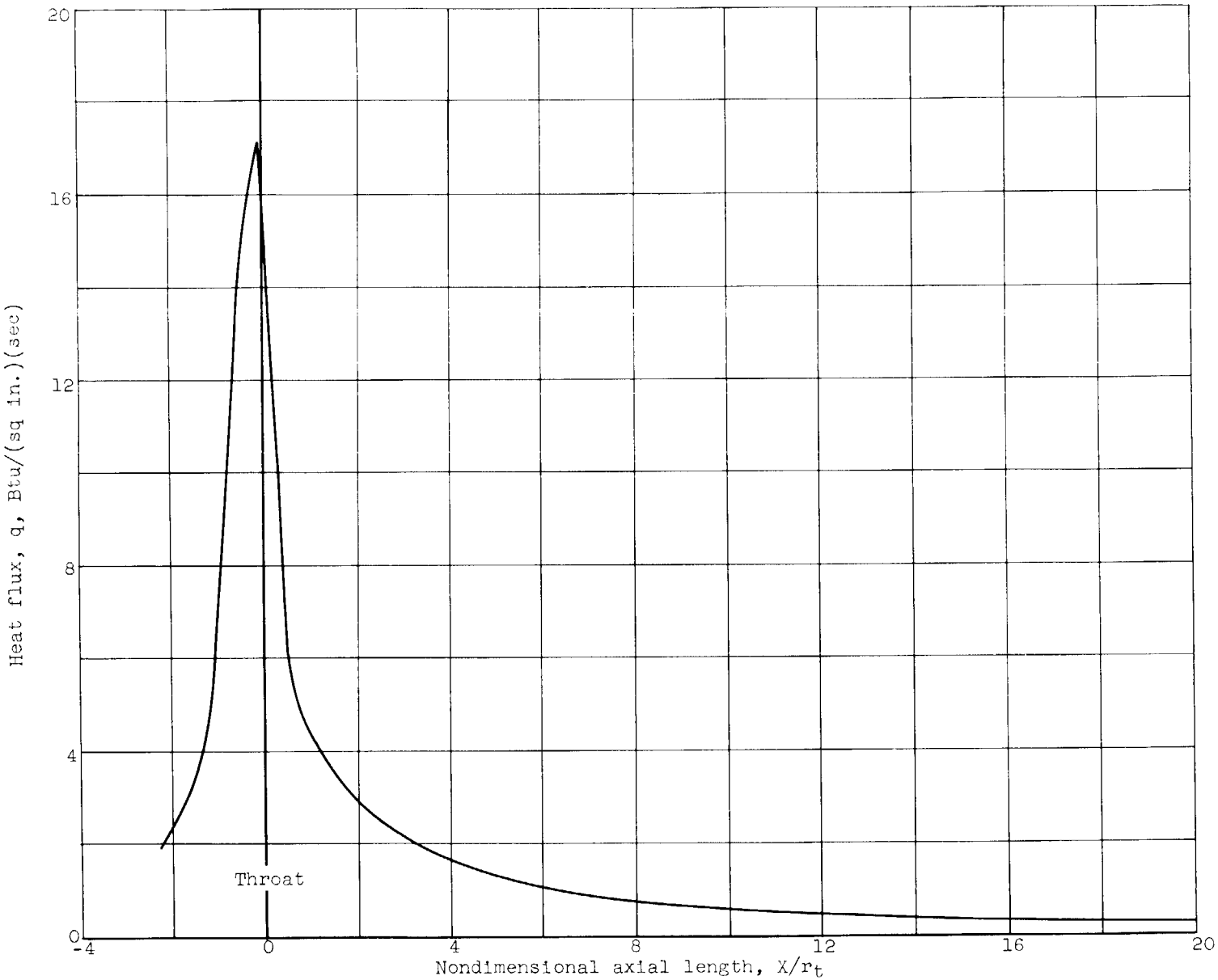

Figure 3. - Typical axial distribution of heat flux in bell-shaped nozzle. Constant wall temperature, 2000° R.

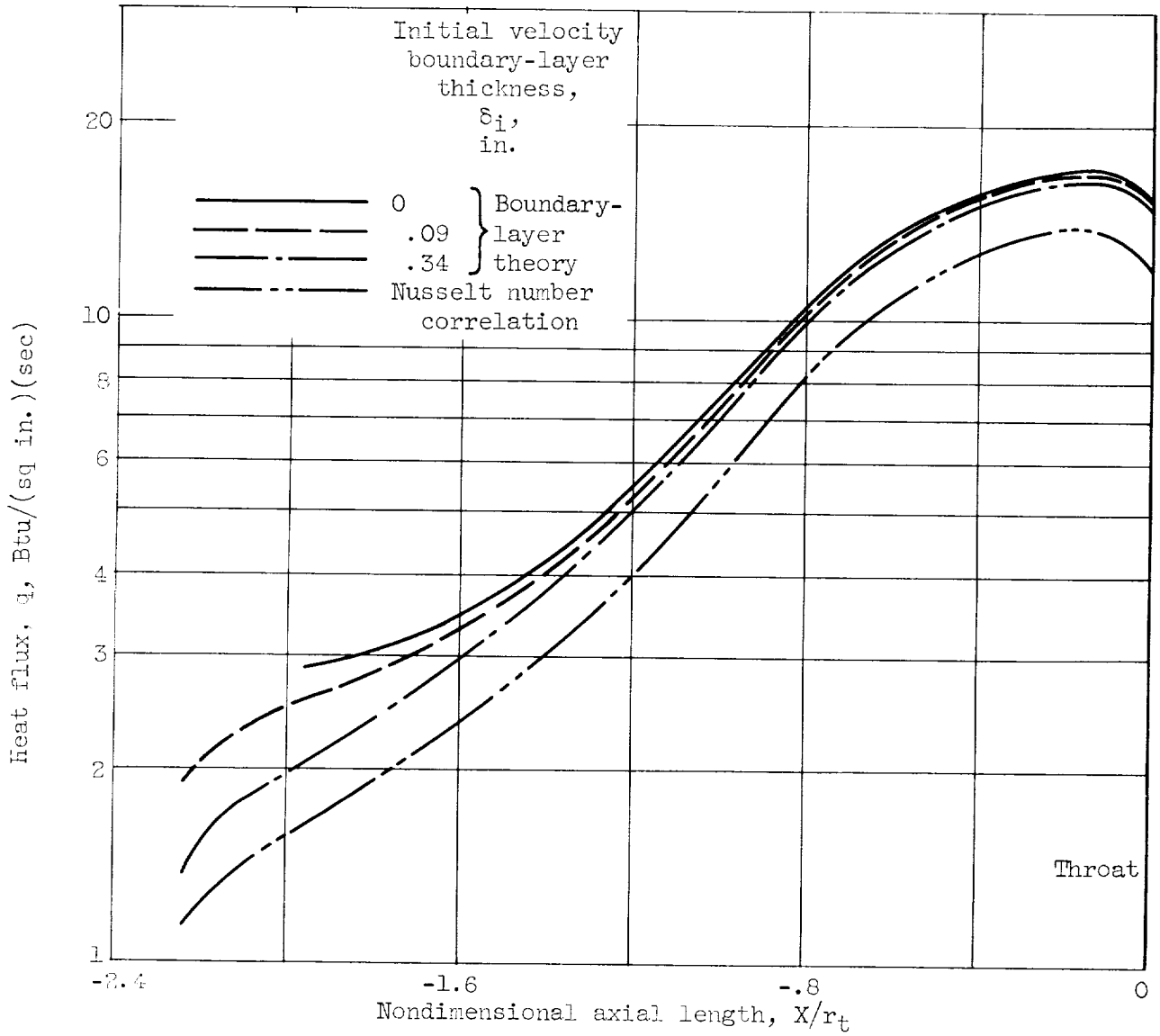

Figure 4. - Axial distribution of heat flux in convergent section of nozzle for various values of initial boundary-layer thickness. Wall temperature, 2000° R.

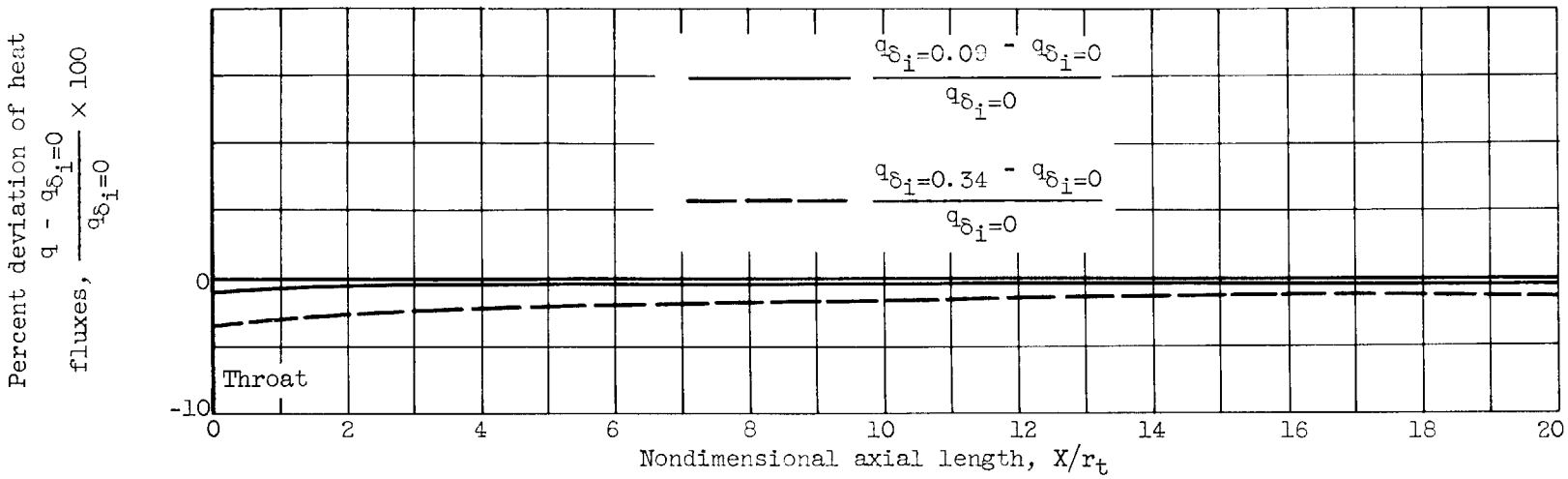

Figure 5. - Effect of initial boundary-layer thickness on heat flux in divergent section of bell-shaped nozzle. Constant wall temperature, 2000° R.

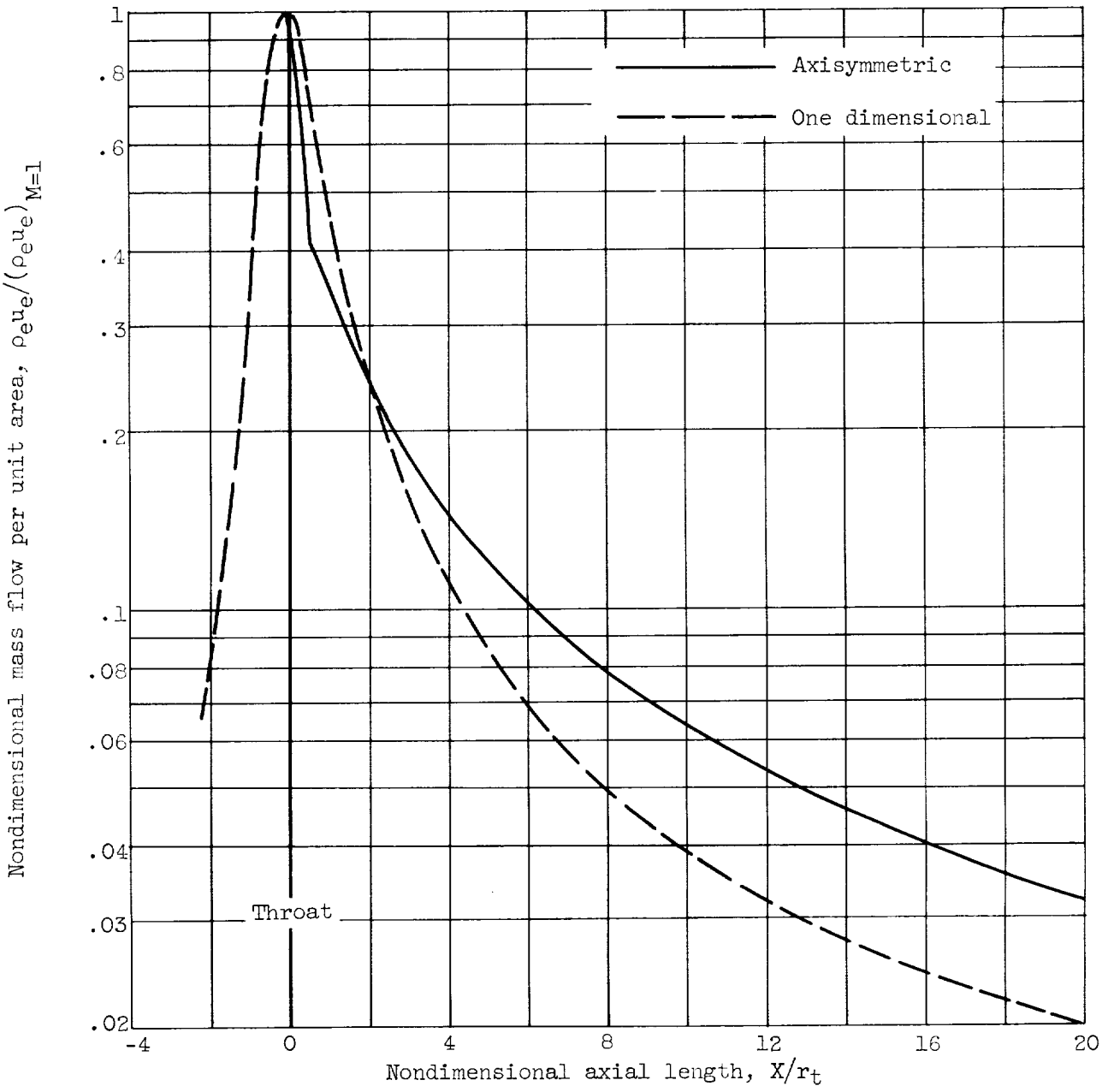

Figure 6. - Axial distribution of nondimensional mass flow per unit area in bell-shaped nozzle.

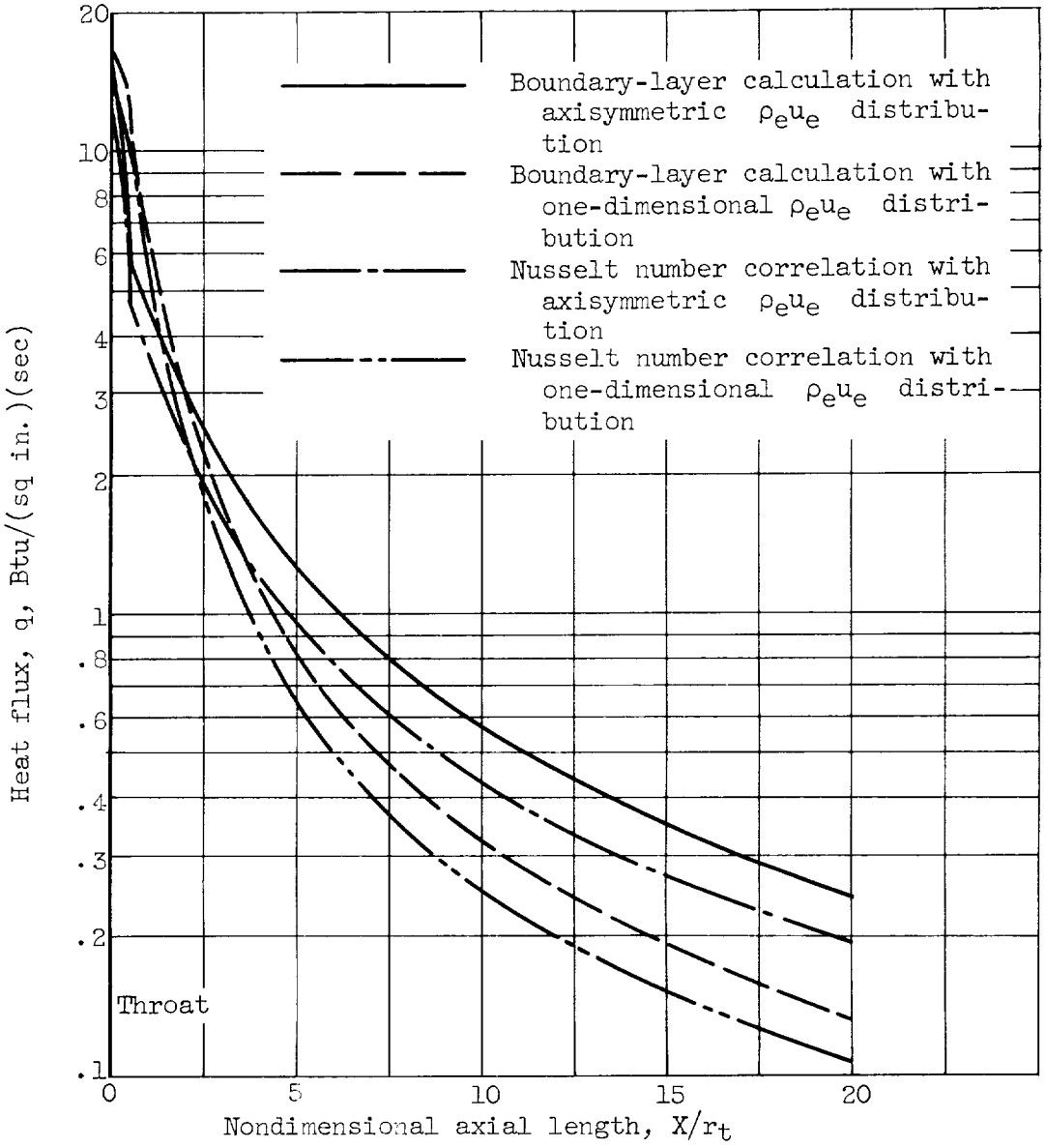

Figure 7. - Comparison of axial distributions of heat flux in divergent section of bell-shaped nozzle. Constant wall temperature, 2000° R.

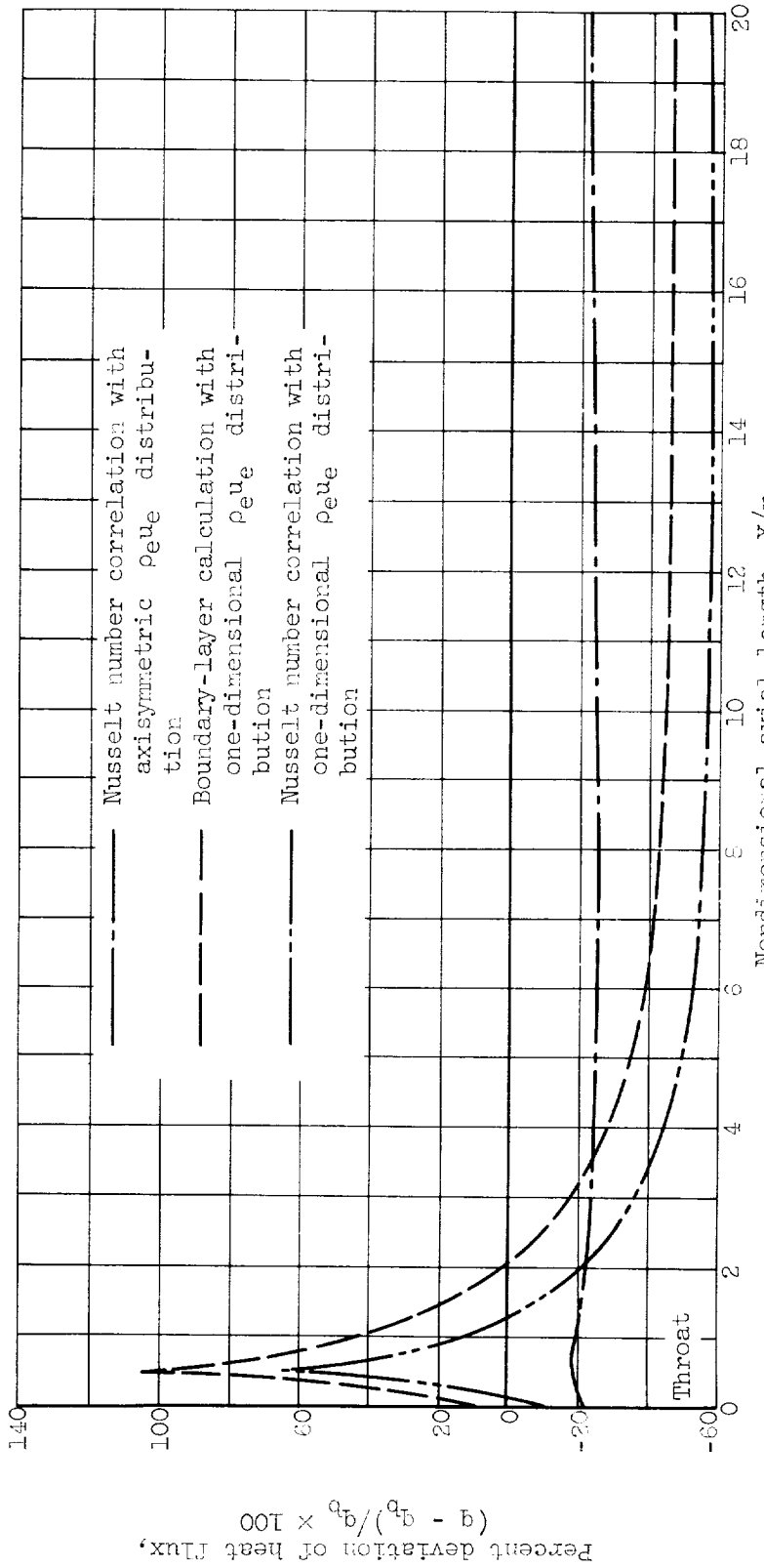

Figure 5. - Comparison of axial distribution of heat flux in divergent section of bell-shaped nozzle. Constant wall temperature, 2000° R.

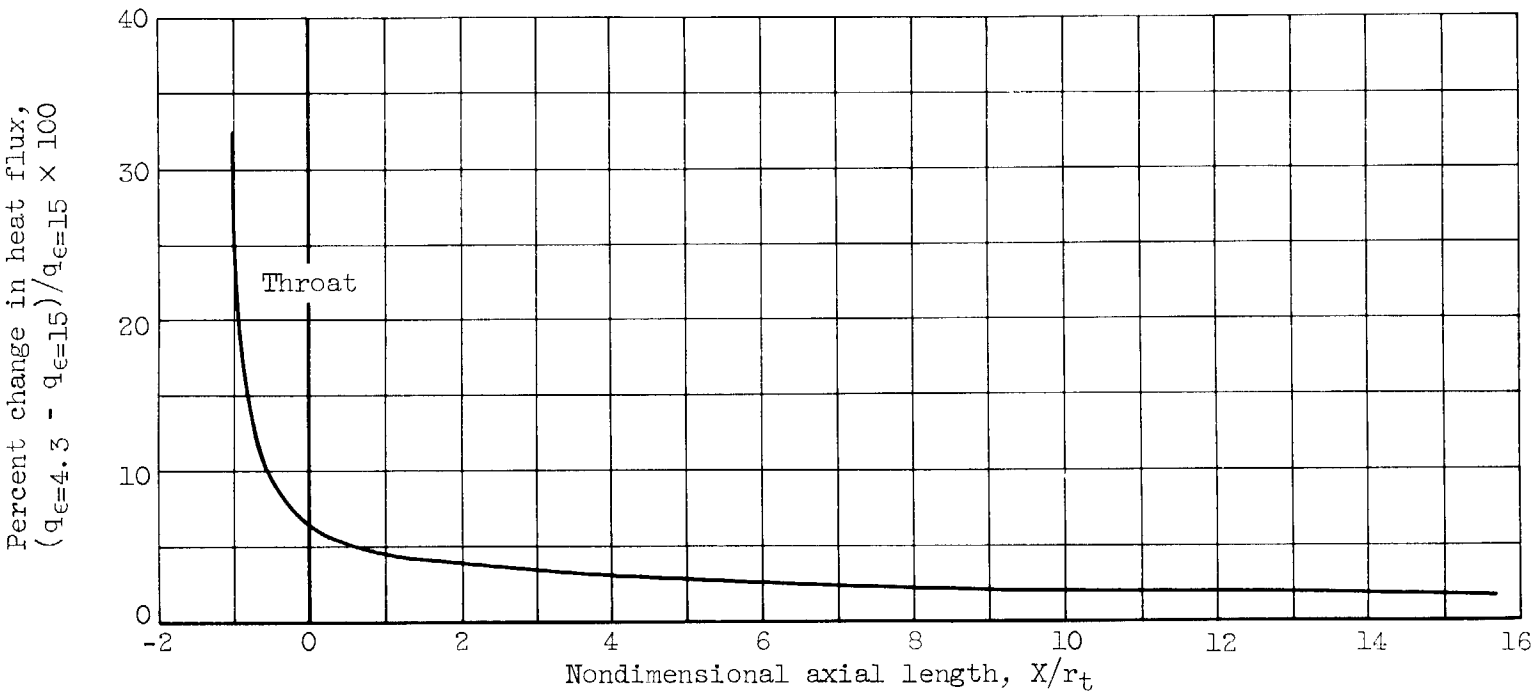

Figure 9. - Variation in heat-flux distribution arising from reduction in contraction ratio from 15 to 4.3.

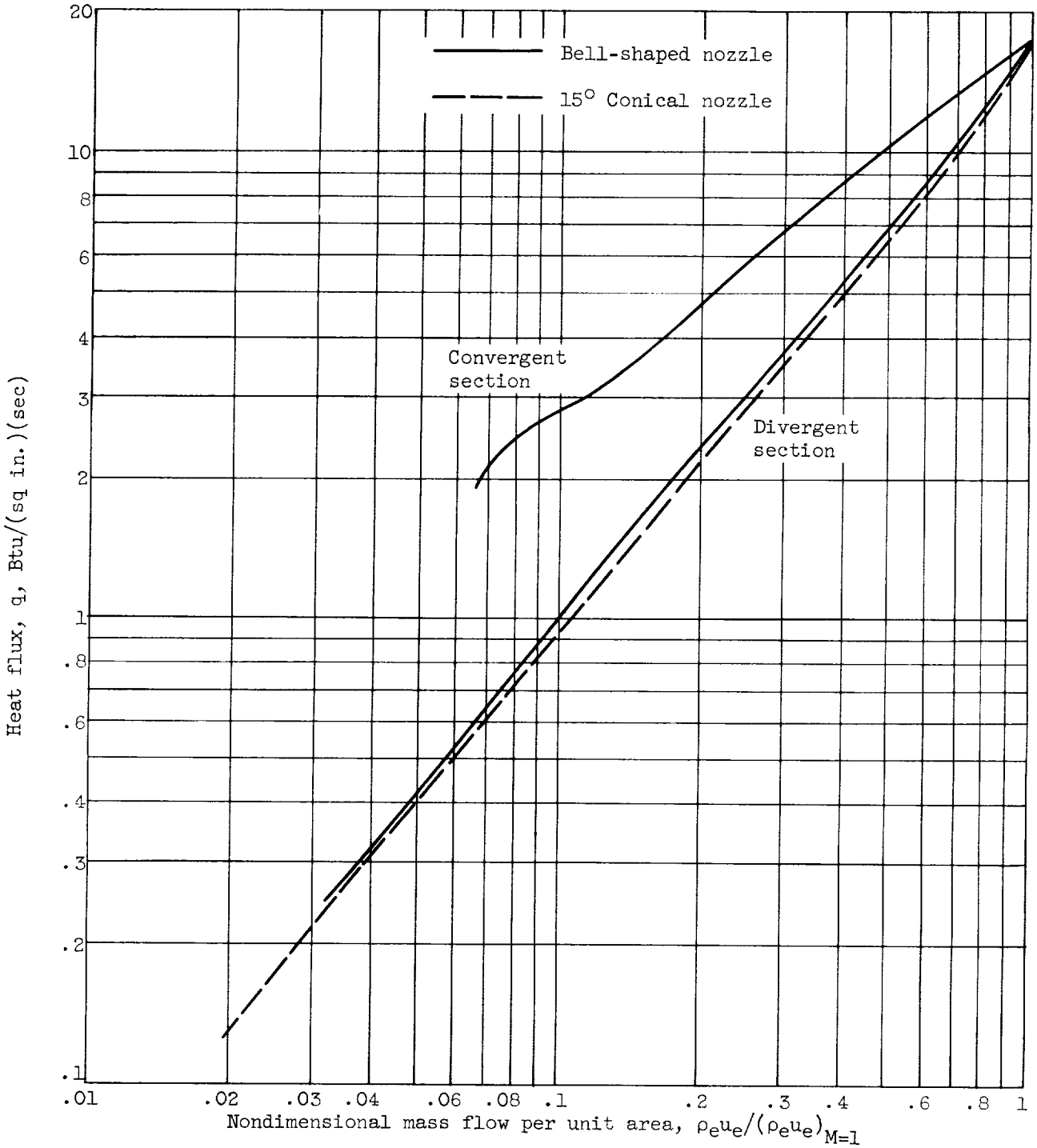

Figure 10. - Comparison of heat-transfer variations with mass flow per unit area for 15° conical and bell-shaped nozzles. Constant wall temperature, 2000° R.

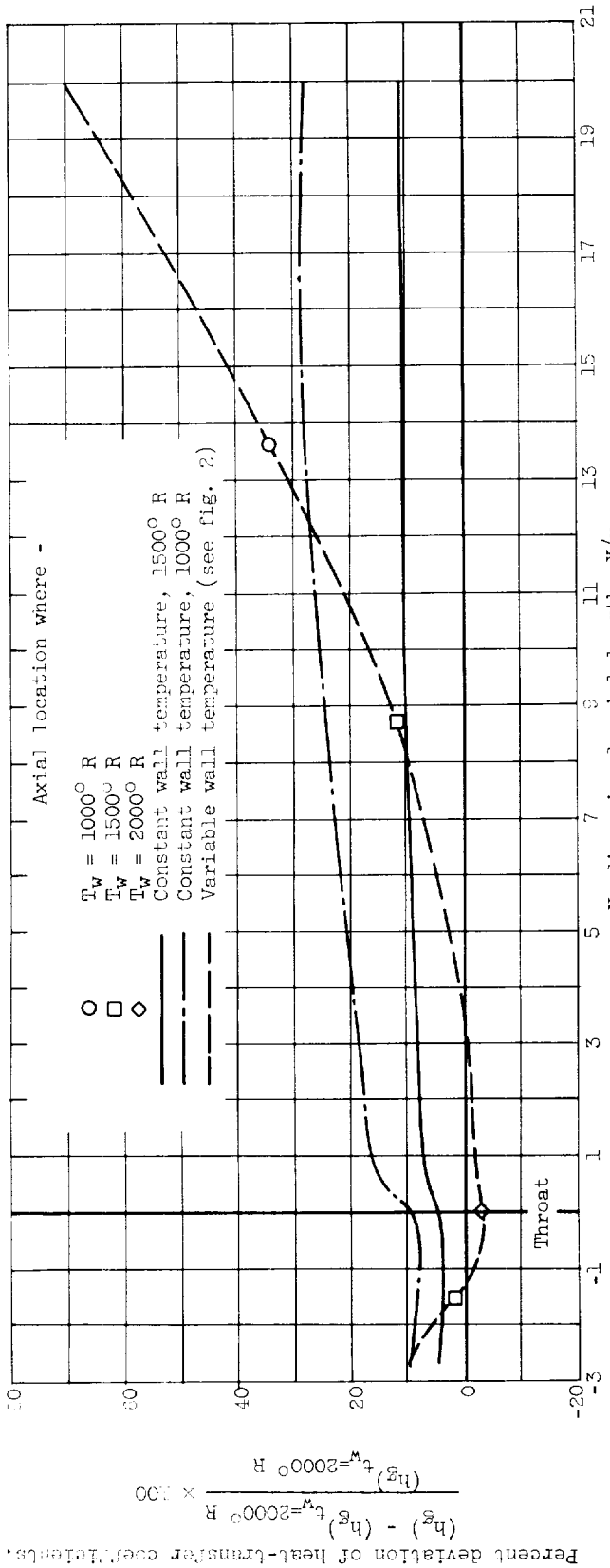

Figure 11. - Effect of wall temperature on axial distribution of heat-transfer coefficient in bell-shaped nozzle.